Position Optimization of Strain Gauge on Blades

ByeongKeun Choi*·HyunSeob Lee*·BoSuk Yang**·Marc P Mignolet***

Key Words : Signal-to-noise ratio, Mispositioning of gauge, The probability of gauge failure, Mistuning

ABSTRACT

This paper focuses on the formulation and validation of an automatic strategy for the selection of the locations and directions of strain gauges to capture at best the modal response of a blade in a series of modes. These locations and directions are selected to render the strain measurements as robust as possible with respect to random mispositioning of the gauges and gauge failures. The approach relies on the evaluation of the signal-to-noise ratios of the gauge measurements from finite element strain data and includes the effects of gauge size. A genetic algorithm is used to find the strain gauge locations-directions that lead to the largest possible value of the smallest modal strain signal-to-noise ratio, in the absence of gauge failure, or of its expected value when gauge failure is possible. A fan blade is used to exemplify the applicability of the proposed methodology and to demonstrate the effects of the essential parameters of the problem, i.e. the mispositioning level, the probability of gauge failure, and the number of gauges.

1. Introduction

Measuring vibrations of turbomachine blades is a substantially harder task than it is for most other structures. The difficulties encountered stem in particular from the harsh operating conditions of the blades, e.g. the rotation, the fluid flow, as well as their structural peculiarities, e.g. sharply peaked modal strain distributions and mistuning effects. In general, the need to not perturb the aerodynamics around the blades and the high centripetal loading they are subjected to limit the choice for blades to strain gauges and, more recently, light probes systems. Further, the rotation of the system considered necessitates the use of a slip ring to transmit the strain gauge signals to the non-rotating environment. It thus restricts the number of these devices to only a few, typically many fewer than the product of the number of modes of interest by the number of blades on the disk.

In general, it would be desirable to instrument a series of blades in order to capture the one yielding the largest resonant response because of the mistuning which incurs dramatic differences in the amplitudes of the resonant response of different blades. Given the limitations of slip rings, the instrumentation of several blades is possible only by using p strain gauges per blade to obtain the modal strain amplitudes of m different modes, and $p < m$.

With such a small number of strain gauges, it is not possible to obtain an accurate perspective of the strain field from the measurements alone. The standard resolution of this issue is then to rely on finite element analyses to obtain the overall shape of the strain field and use the measurements as scale factor of the computational results. To achieve the largest accuracy given the inherent gauge error, quantization noise, etc., it would best to position the strain gauges at the peaks of the strain distribution of the different modes considered. Indeed, the peaks of the strain distribution are often very sharp and a slight mispositioning of the strain gauge, in location and/or direction, may result in a measured strain much less than the maximum value. The location of the strain gauges thus appears as a compromise between high strain levels and low sensitivity to mispositioning.

Another important practical consideration that affects the selection of the strain gauge locations is their potential failure. The combination of the large centripetal loading, the entraining fluid flow, and possibly high temperatures represents a particularly harsh environment in which it is not unusual that a strain gauge debonds. The optimization of strain gauge placement must then include also the potential loss of one or several of the strain gauges.

Surprisingly, given the practical importance of this issue, there has been only a few investigations focusing on the positioning of strain gauges on blade.(1-3) Therefore, the approach proposed in this paper is complementary of these earlier efforts as it is statistical in nature considering the random effects of mis-positioning and gauge failure on the measured strains.

2. The Max-Min-Max Principle

2.1 No Gauge Failure

In the absence of gauge failure, the selection of the strain gauge locations is dictated by the modal strain distribution and by the measurement noise and potential mispositioning of the gauges. While the noise and mispositioning do not affect the strain measurements in similar manners, they have one common effect, i.e. to

* Gyeongsang National University
E-mail : bgchoi@nongae.gsnu.ac.kr
Tel : (055) 640-3059, Fax : (055) 640-3188

** PuKyong National University

*** Arizona State University

produce variability in the obtained strain values. The quantification of the variability present is most conveniently achieved through the signal-to-noise ratio (*SNR*) which is defined as

$$SNR(\varepsilon) = \mu_\varepsilon / \sigma_\varepsilon \quad (1)$$

In this equation, μ_ε denotes the mean value of the strain. Further, σ_ε represents the corresponding standard deviation which involves the contributions of the noise (σ_ε^n), and of the mispositioning (σ_ε^m).

From its definition, Eq. (1), the *SNR* can be viewed as a measure of confidence on the observed strains, i.e. the larger this value is the smaller the variability is in relation to the strain level. On this basis, the overall strain gauge placement strategy proposed here focuses on maximizing the *SNR*. The specifics of the optimization approach are dependent on how the measurements are used to estimate the modal strain distributions. In the present effort, it has been assumed that the scaling factor of the finite element results for a specific mode are evaluated from the gauge yielding the largest *SNR* of all *p* gauges for that mode. That is, let $SNR(i, j, \underline{X})$ be the *SNR* of the measurement at location *i* in the *j*th mode of response when the gauges are located at coordinates $\underline{X}$. Then, the best estimate of the forced response in that mode will be obtained from the gauge *i* that gives the largest value of $SNR(i, j, \underline{X})$ so that the *SNR* of the response in the *j*th mode is

$$SNR(j, \underline{X}) = \max_i SNR(i, j, \underline{X}) \quad (2)$$

The appropriateness of a given set $\underline{X}$ of strain gauge locations can then be characterized by the values $SNR(j, \underline{X})$, j = 1, 2, ..., m, and more succinctly by the lowest of these *SNR* taken over all modes considered, i.e.

$$SNR(\underline{X}) = \min_j SNR(j, \underline{X}) \quad (3)$$

On this basis, it is proposed here to select the strain gauge locations $\underline{X}$ to maximize $SNR(\underline{X})$. This process results in the following max-min-max optimization principle

$$\textbf{Maximize} \; \min_j \left\{ \max_i \left[SNR(i, j, \underline{X}) \right] \right\} \quad \textbf{with respect to} \; \underline{X} \quad (4)$$

2.2 Multiplicity of Solutions

It should be noted that the max-min-max optimization problem stated above quite often yields a multiplicity of solutions that tends to grow as the number of gauges increases. This multiplicity of solution is most clearly seen when the number of gauges equals the number of modes. In this case, the solution that would be expected from the optimization is the one in which each gauge is placed at the peak location of the *SNR* of a different mode. The corresponding value of the objective function, i.e. $SNR(\underline{X})$ is the smallest of the peak modal *SNR* on the blade. Let that value be *S* and the corresponding gauge location-direction be $\underline{X}_s$. Denote also by *d* the mode in which *S* is achieved. Then, a series of solutions exists each of which yields the same best min-max *SNR S*. These different solutions can be constructed as follows. First, select $\underline{X}_s$ as the first gauge location-direction. Then, select the second gauge location-direction to provide a *SNR* of mode 1 (if $d \neq 1$, mode 2 otherwise) larger than *S*. Similarly, choose the third gauge location-direction to yield a *SNR* of mode 2 (if $d \neq 2$, mode 3 otherwise) that is larger than *S*, etc. In this fashion, the minimum of the modal *SNR* will be the best possible value, *S*, irrespectively of the exact locations-directions of the gauges 2, 3,..., $p = m$.

The multiplicity of solutions can be resolved by turning to an objective function that involves *SNR* of all gauges, e.g. a weighed average across different gauges. However, the smallest of the modal *SNR* obtained for such objective functions is often much smaller than the one obtained with the max-min-max principle as weighted average objective functions can be biased by large values of the *SNR* of some mode at the detriment of one or several others.

To resolve the multiplicity issue within the max-min-max framework, it was decided to proceed with a sequential optimization approach the first step of which is the one described above. Once the largest minimum modal *SNR* has been identified, the corresponding location-direction is held for gauge 1. The max-min-max optimization process is then repeated to maximize the *second* smallest modal *SNR* of the combined *p* gauges (including the fixed first one). If, at the completion of this second step, it is found that the second smallest modal *SNR* is also obtained by gauge 1, the third smallest modal *SNR* is then considered. The process is repeated in this fashion until all gauge locations-directions have been selected.

2.3 Potential Gauge Failure

The failure of a gauge is a random event that leads to a loss of measurement and thus to zero *SNR* for the failed gauge. In general, this sudden change of *SNR* values of a gauge will also affect the overall *SNR* of Eq. (2), (3) rendering them random variables depending on the state, failed or intact, of the gauges. The optimization problem of Eq. (4) is then no longer well posed and will be replaced by the maximization of the *expected value* of $SNR(\underline{X})$, i.e. the average *SNR* that would be observed in a series of identical tests with gauges randomly failing or staying intact. Denoting by P_f the probability of failure of a gauge and assuming that the state (failed/intact) of different gauges are statistically independent random variables, it can be shown that

$$E\left[\min_j \left\{\max_i \left[SNR\left(i, j, \underline{X}\right)\right]\right\}\right] = \left(1 - P_f\right)^p SNRmM^{(p)} + P_f\left(1 - P_f\right)^{p-1}\left[\sum_{l=1}^{p} SNRmM_l^{(p-1)}\right] + P_f^2\left(1 - P_f\right)^{p-2} \left[\sum_{\substack{k,l=1\\ k\neq l}}^{p} SNRmM_{kl}^{(p-2)}\right] + \cdots \tag{5}$$

where $E[\bullet]$ is the expected value operator. Further, $SNRmM^{(p)}$ denotes the smallest of the modal *SNR* of the intact strain gauges set, i.e. as computed from Eq. (4). Similarly, $SNRmM_l^{(p-1)}$ is also the smallest modal *SNR* but for the set of p-1 strain gauges remaining after the lth one has failed. Next, $SNRmM_{k,l}^{(p-2)}$ is the smallest modal *SNR* for the set of p-2 strain gauges remaining after the kth and lth ones have failed, etc.

Note that the value of the above expected *SNR* is a function of the *SNR* of all gauges, at the contrary of Eq. (3). The multiplicity of solutions discussed in connection with the no gauge failure case is thus removed by considering the probability of gauge failure.

It should be noted that Eq. (5) has been obtained under the assumption of an equal probability of failure for all gauges but it is readily extendable to the situation where this probability varies with gauges, e.g. is dependent on either the gauge number or its location on the blade.

3. Optimization Algorithm

The proposed strain gauge placement strategy is based on the selection of the locations-directions on the blades that yield a best *SNR*. This process was accomplished in two stages. First, a search over a discrete set of locations and directions was conducted to find the best positioning of the strain gauges within this set. Then, if desired, a more refined positioning could be accomplished by allowing the strain gauge to be located in the neighborhood of the optimum solution corresponding to the discrete set.

The discrete set of locations and directions was obtained by considering each internal node and a series of equidistant angles from 0° to 180°. Accordingly, a very large discrete set was obtained in which many local maxima of the *SNR* could be expected. To ease computations, a set size reduction was first performed. Specifically, consider two different locations and directions each having it's own set of *SNR*. If the *SNR* of the second location-direction are lower than the corresponding values for the first one then the second location-direction cannot be part of the optimum solution. Thus, the second location-direction can be removed from the set to be investigated.

To address the optimization effort given the large number of local maxima expected, it was decided to use the simple genetic algorithm which had successfully been used in an optimization of intentional mistuning patterns[4].

It may be desired in some circumstances to dispose of a finer positioning capability than that provided by the finite element mesh. Such a freedom can be obtained by proceeding first with the search through the discrete set, as described above, and using the optimum locations and directions thus found as an initial condition for a refined optimization. While the *SNR* computations could be carried out as described above, an alternate approach was implemented in which the *SNR* were directly interpolated from their values at the nodes surrounding the optimum locations. For this task, the Lagrangian interpolation polynomial was used and the optimization process was implemented in the MATLAB(v5.0) environment with the function constr. The extrapolation of the *SNR* from the neighboring nodes to the border or corner did seem to be fairly well conditioned.

4. Example

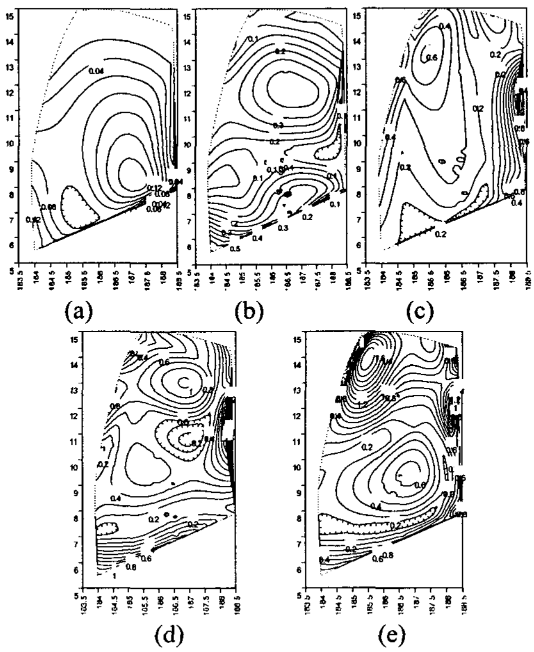

Fig. 1 Modal strain distributions for the first 5 modes of the fan blade (Pressure side)

To demonstrate the application of the proposed robust positioning of strain gauges, a fan blade from a Honeywell engine was considered. The ANSYS finite element consisted of 4,830 8-node blocks, 7,560 nodes, and the first 5 modes were considered. The strain distributions on the pressure side of the blade are shown in Fig. 1 (a)-(e) for each of these 5 modes. The discrete set of locations-directions was formed by the 4,624 internal nodes of the pressure and suction sides and 36 different angles (5° apart). Accordingly, there were a total of 166,464 considered locations and angles to position the strain gauges. The modal *SNR* of the 5 modes were computed at each of these locations-directions. The standard deviation of mispositioning (in position only, not in angle) was varied from 0.01 in. (0.254 mm.) to 0.12 in. (3.048 mm.). The largest *SNR* value obtained for each mode is shown in Fig. 2. Note the difference in behavior exhibited by modes 1 and 5 as compared to 2 and 3.

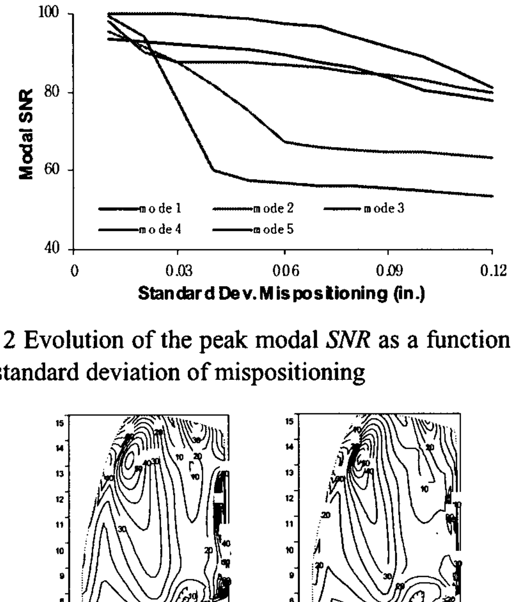

Fig. 2 Evolution of the peak modal *SNR* as a function of the standard deviation of mispositioning

(a) (b)

Fig. 3 Distribution of *SNR* on the pressure side of the blade for the third mode and for a standard deviation of mispositioning in location only of (a) 0.03in, and (b) 0.06 in.

For the former modes, the peak *SNR* decreases slowly and smoothly as a function of the mispositioning level. On the contrary, for modes 2 and 3, there is initially a rapid decrease of *SNR* but this trend suddenly changes and an almost constant behavior is observed. To understand these trends, the distribution of *SNR* on the blade was analyzed, e.g. see Fig. 3(a) and (b). As done in connection with the strain distributions of Fig. 1, these figures were obtained by keeping for each location on the blade the largest *SNR* computed as the angle was varied through its 36 different values. Note from Fig. 3(a) and (b) that the *SNR* distribution exhibits, as the corresponding strain distribution of Fig. 1(c), two dominant peaks, one very close to the trailing edge and on toward the leading edge. For the smaller mispositioning level, 0.03 in. see Fig. 3(a), it is the sharp trailing edge peak that yields the largest *SNR* while thesituation is reversed for the 0.06 in. mispositioning of Fig. 3(b). Note from Fig. 2 that the 0.03 in. mispositioning level is in the rapidly decaying zone while the 0.06 in. case falls in the flat region of the curve. An analysis of the *SNR* distribution plots for 0.04 in. and 0.05 in. mispositioning levels demonstrates that in fact the break in the curve of Fig. 2 does occur when the peak *SNR* shifts from one maximum (trailing edge) to the other (leading edge). The different rates of decay of the *SNR* with mispositioning level before and after the break can be understood from the strain distribution plot of Fig. 1(c). Specifically, since the trailing edge peak is very sharp, mispositioning will greatly affect the measured strains and thus the *SNR* will rapidly decrease with increasing mispositioning. On the contrary, since the leading edge peak is quite blunt, mispositioning will only produce a mild effect as seen by the almost flat zone of Fig. 2. A similar situation occurs for mode 2 but also for mode 1 but it is not seen in Fig. 2 because the shift occurs at a mispositioning level below 0.01 in. Indeed, the strain distribution for mode 1, see Fig. 1(a), exhibits two almost equal peaks both on the pressure side with the largest one at the root of the blade on the leading edge. Note that the *SNR* peak shifting explains in particular why the curve of Fig. 2 for mode 1 does not seem to converge to 100 at 0 mispositioning as required from the 1% measurement noise.

These first results support the choice of the *SNR* as the appropriate metric for the selection process of gauge location-direction. Thus, the max-min-max principle is expected to follow the intuitive rule of selecting the peak strain location if the peak is not "too sharp" but it will quantify at what mispositioning level the shift in location-direction must take place.

Having validated the usefulness of the *SNR* for the gauge positioning process, the optimization of the minimum modal *SNR* was undertaken, first without gauge failure, then with a nonzero probability of such an event. It was first observed that the simple two-pass reduction strategy was particularly effective in reducing the number of locations-directions to be considered. For a 0.06 in. standard deviation of mispositioning, the set size was reduced from 166,464 locations-directions to

5,020 or 3% of the original size!

While genetic algorithms have a series of advantages over traditional gradient-based techniques, they are also known to occasionally suffer from a lack of convergence to the absolute optimum. It was thus desired to first assess the convergence behavior of the genetic algorithm. The two limiting cases of 1 and 5 gauges were thus considered first. The optimum for 1 gauge could easily be obtained by an exhaustive search through the 5,020 directions-locations. Further, the 5 gauges optimum solution was also readily determined as it corresponds to the gauges being located on the peaks of the 5 modal *SNR* distributions. In both cases, the genetic algorithm recovered exactly the expected optimum solution. The optimum positioning of 2, 3, and 4 gauges was then considered and the corresponding modal *SNR* are shown in Fig. 4. It is seen from this figure that an increase in the number of gauges leads, as expected, to a monotonic increase in all modal *SNR*. However, the objective function, i.e. the minimum modal *SNR* appears to be rapidly converging, i.e. it is almost constant for 3 or more gauges. Certainly, the consideration of 4 or 5 gauges leads to improvements but only on modes (e.g. 1, 4, and 5) that are already well captured as they exhibit large modal *SNR*. From a pragmatic point of view, the return on investment is low for more than 3 gauges for 5 modes, a result that appears to match some practical experience. These results also demonstrate that the max-min-max principle has forced the efficient use of the strain gauges and thereby validate its use.

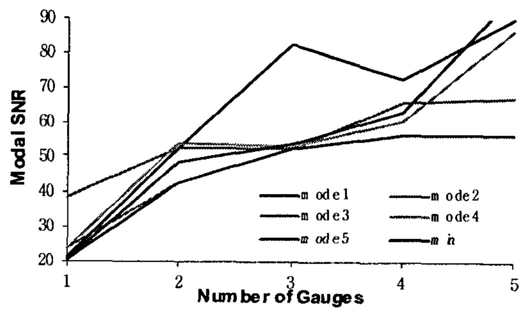

Fig. 4 Evolution of the modal *SNR* ratios as a function of the number of strain gauges, standard deviation of mispositioning = 0.06 in. P_f= 0.

The influence of potential strain gauge failure was considered next for 3 gauges and a mispositioning standard deviation of 0.06 in. Beside the case P_f = 0 treated above, the values 0.1, 0.2, and 0.3 were also considered. Intuitively, it is expected that the possibility of gauge failure should promote the evenness of the *SNR* of the gauges across the different modes. To validate or invalidate this expectation, the *SNR* of the 3 gauges for the 4 different probabilities of failure were plotted as a function of the mode number, see Fig. 5. This figure does indicate some trend of increase of the smallest *SNR* and decrease of the largest one as the probability of failure increases but this trend is certainly not as clear as intuitively thought. In this regards, it should be recognized that (1) not all *SNR* are present in the objective function, i.e. the expected minimum modal *SNR*, only 7 of the 15 values appear in Eq. (5) and (2) the *SNR* that are present in Eq. (5) are not equally weighted.

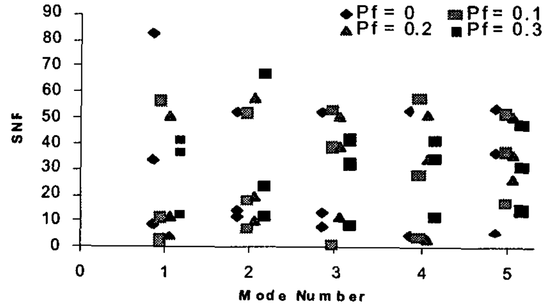

Fig. 5 *SNR* for 3 gauges as a function of the mode number for different probabilities of failure

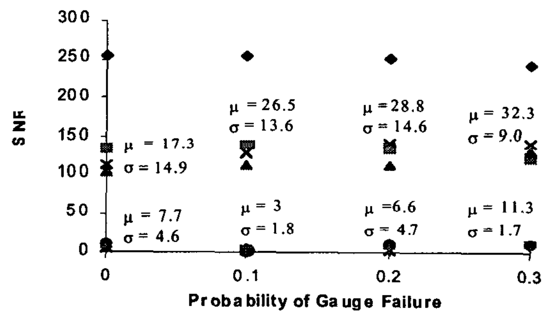

Fig. 6 Minimum modal *SNR* corresponding to the optimum solutions for 3 gauges as functions of the probability of gauge failure.

In light of these observations, it was decided to reprocess the data of Fig. 6 emphasizing only the 7 *SNR* of Eq. (5) and considering separately $SNRmM^{(p)}$, the 3 $SNRmM_l^{(p-1)}$ values, and the 3 $SNRmM_{k,l}^{(p-2)}$ terms. To display these *SNR* on the same plot while separating them, arbitrary shifts of 200(the top level, all three gauge intact) and 100(one gauge failure) were added respectively to $SNRmM^{(p)}$ and the 3 terms $SNRmM_l^{(p-1)}$. The result of this process is Fig. 6. Several important observations can be drawn from this plot.

First, as the probability of failure remains small, the dominant contribution to the objective function is still the minimum modal *SNR*. Thus, this value (the diamonds of Fig. 6) only slightly decreases at first. Thus, the consideration of a probability of failure as large as 0.2 does not significantly alter the reliability of the measured strains if failure does not occur. On the contrary, if failure does occur once, the mean smallest modal *SNR* decreases from 28.8 for the optimal solution considering $P_f = 0.2$ to 17.3 for the one obtained with $P_f = 0$. This drop is equivalent to an increase by 66% of the measurement error on the strains, from 1/28.8 = 3.5% to 1/17.3 = 5.8%. It thus appears in this case that the safe approach, i.e. to consider a potential gauge failure even when it is unlikely, is appropriate if the probability of gauge failure is 0.2 or less. For higher values of this probability, the optimal solution becomes overly conservative and the accuracy of the measured strains is affected.

Consider next the *SNR* obtained with one failed gauge, i.e $SNRmM_l^{(p-1)}$. It is found from Fig. 6 that these values increase monotonically on average and that their standard deviation (variability) decreases as the probability of failure increases. Thus, the optimum solution is driven to yield a minimum modal *SNR* that is (1) fairly high, (2) quite insensitive to which gauge has failed. This behavior is in fact the evenness expected above.

Finally, although the *SNR* obtained with two failed gauges, $SNRmM_{k,l}^{(p-2)}$, do not affect significantly the objective function for the low probabilities of failure considered, it is nevertheless seen from Fig. 6 that these terms do exhibit the behavior of increasing mean and decreasing standard deviation already observed in connection with $SNRmM_l^{(p-1)}$. The clarity of the trends shown in Fig. 6 as opposed to the rather unclear ones of Fig. 5 demonstrates that the strain gauge positioning strategy with potential gauge failure is intuitively simple and logical but that obtaining the optimal solution without an efficient search algorithm is not.

The effect of the gauge size on the optimum strain gauge placement was investigated by considering a square gauge of 0.06 in. with standard deviations of mispositioning equal to 0.03 in. and 0.06 in. In both cases, it was found that the distribution of *SNR* was almost identical to the one obtained by a zero-size gauge and thus no change in the optimal gauge locations-directions was observed.

The convergence of the strain gauge locations-directions was achieved very quickly and remained within the neighborhood of the solution provided by the genetic algorithm and used as initial condition.

5. Summary

This paper focused on the formulation and validation of an automatic strategy for the selection of the locations and directions of strain gauges to capture at best the modal response of a blade in a series of modes. The approach seeks the strain gauge locations-direction that lead to the maximum robustness (*SNR*) of the measured strain values with respect to the inherent system measurement noise and the mispositioning of the gauge in location and direction.

The formulation of a multi-step optimization strategy is used to search for the best strain gauge locations-directions in this paper. The first step of the approach is a simple but efficient reduction strategy that eliminates locations and directions which cannot be optimal solutions. The second step is a true optimization effort based on a genetic algorithm and aims at the best placement of strain gauges on the nodes of the finite element mesh. The final step is a fine optimization that searches for the optimal placement of the strain gauges within the finite elements. The proposed strategy for the selection of strain gauge locations-directions was finally exemplified and validated on a full finite element model of a fan blade. The trends of the optimal strain gauge locations were found to be in complete agreement with intuitive expectations but were able to *quantify precisely* the effects of mispositioning and gauge failure.

Acknowledgements

The support of this work by the Brain Korea 21 Project is gratefully acknowledged.

References

(1) Yang, M.-T, and Griffin, J.H., 1998, "Theory and Methodology of Optimally Measuring Vibratory Strains in Closely Spaced Modes," *Journal of Engineering for Gas Turbines and Power*, **120**, No. 4, pp. 801-807.

(2) Sensmeier, M.D., and Nichol, K.L., 1998, "Optimum Placement of Sensors for Vibration Measurements on Turbine Engine Blades," *Proceedings of the 39th AIAA/ASME/ASCE/AHS/ASC Structures, Structural Dynamics, and Materials Conference,* Long Beach, CA, Apr. 20-23, AIAA Paper 98-1849.

(3) Sensmeier, M.D., and Nichol, K.L, 2000, "Improved Vibration Monitoring Through Optimization of Sensor Placements," *Presented at the International Gas Turbine & Aeroengine Congress and Exposition,* Munich, Germany, May 8-11, ASME Paper 2000-GT-612.

(4) Choi, B.-K., Lentz, J., Rivas-Guerra, A.J., Mignolet, M.P., 2001, "Optimization of Intentional Mistuning Patterns for the Reduction of the Forced Response Effects of Unintentional Mistuning," *Presented at the Turbo Expo 2001*, New Orleans, Louisiana, Jun. 4-7, Paper 2001-GT-0293. *Journal of Engineering for Gas Turbines and Power,* to be Appear.